Frequency of large volcanic eruptions over the past 200,000 years

Eric W. Wolff[1], Andrea Burke[2], Laura Crick[2], Emily A. Doyle[1], Helen M. Innes[2], Sue H. Mahony[3], James W.B. Rae[2], Mirko Severi[4] and R. Stephen J. Sparks[3]

[1]Department of Earth Sciences, University of Cambridge, Cambridge CB2 3EQ, United Kingdom
[2]School of Earth & Environmental Sciences, University of St Andrews, St Andrews, KY16 9AL, United Kingdom
[3]School of Earth Sciences, University of Bristol, Bristol BS8 1RJ, United Kingdom
[4]Chemistry Department, University of Florence, Sesto F.no (FI) 50019, Italy

Correspondence to: Eric W. Wolff (ew428@cam.ac.uk)

Abstract. Volcanic eruptions are the dominant cause of natural variability in climate forcing on timescales up to multidecadal. Large volcanic eruptions lead to global-scale climate effects and influence the carbon cycle on long timescales. However, estimating the frequency of eruptions is challenging. Here we assess the frequency at which eruptions with particular deposition fluxes are observed in the EPICA Dome C ice core over the last 200 kyr. Using S isotope analysis we confirm that most of the largest peaks recorded at Dome C are from stratospheric eruptions. The cumulative frequency through 200 kyr is close to linear suggesting an approximately constant rate of eruptions. There is no evidence for an increase in the rate of events recorded in Antarctica at either of the last two deglaciations. Millennial variability is at the level expected from recording small numbers of eruptions, while multimillennial variability may be partly due to changes in transport efficiency through the Brewer-Dobson circulation. Our record of events with sulfate deposition rates > 20 mg m^{-2} and >50 mg m^{-2} contains 678 and 75 eruptions respectively over the last 200 kyr. Calibration with data on historic eruptions and analysis of a global Quaternary dataset of terrestrial eruptions indicates that sulfate peaks with deposition rates > 20 mg m^{-2} and >50 mg m^{-2} correspond to explosive eruptions of magnitude ≥ 6.5 and ≥ 7 respectively. The largest recorded eruption deposited just over 300 mg m^{-2}.

1. Introduction

Volcanic eruptions can have devastating local effects, and at a global scale they are one of the important natural components of forcing in the climate system (Robock, 2000). The forcing arises from sulfate aerosol that is formed from SO_2 erupted into the stratosphere. On longer timescales the balance between volcanism and weathering controls the CO_2 content of the atmosphere, and changes in volcanic eruption frequency could contribute to the changes in CO_2 concentration observed at glacial terminations (Huybers and Langmuir, 2009). In order to constrain changes in forcing by volcanic aerosol, as well as any role of volcanoes in glacial-interglacial CO_2 change, a key question is whether global eruption rate is steady and, if not, whether any variation is related to climate.

There has been much interest in the notion that rates of explosive volcanism have been moderated by processes related to climate change (Kutterolf et al., 2019; Watt et al., 2013). Rates of mantle melting are expected to be affected by glacial cycles:

melting of ice caps leads to unloading, enhanced mantle melting and enhanced volcanism (Huybers and Langmuir, 2009; Jull and McKenzie, 1996). Rates of volcanism might also be affected by sea level change (Huybers and Langmuir, 2009; Kutterolf et al., 2019). Over very long timescales, changes in plate tectonics and occurrence of mantle plume volcanism are expected to be reflected in rates of volcanism.

Beyond the period of direct historic observations, explosive eruptions are recorded as tephra deposits in terrestrial and marine records, and as both sulfate and occasional tephra deposits in ice cores. Terrestrial tephra deposits give information about location as well as strength and frequency of eruptions (Brown et al., 2014), but they are notoriously difficult to use, and a statistical approach is needed to turn them into useful measures of eruption frequency (Rougier et al., 2018). Tephra in marine cores offers a further opportunity to compile eruption statistics (Mahony et al., 2020), but it is also challenging to compile a record that is unbiased over time and space. Eruptions are also recorded as sulfate deposition in ice cores. While this provides no direct information on the location and magnitude of each eruption, it can be used to log eruptions relevant for climate forcing (Gao et al., 2008; Sigl et al., 2015). There have been only limited investigations (Castellano et al., 2005; Castellano et al., 2004; Cole-Dai et al., 2021; Lin et al., 2022) to estimate volcanic eruption occurrence from ice core data beyond the last 2500 years.

Although records from both poles may be combined to identify explosive eruptions recorded at both poles (and therefore most likely having reached the stratosphere), the use of Greenland ice core records alone is complicated, because they are dominated by the relatively local input from Icelandic eruptions. For the region around Antarctica, ~~has rather few local eruptions~~there are active volcanoes in New Zealand, the Andes, the South Sandwich and South Shetland Islands, and within the continent in Marie Byrd Land and around McMurdo Sound. However the frequency of large eruptions from these areas is expected to be low (notwithstanding an unusual event at the last deglaciation (McConnell et al., 2017)), and the local sources within the continent are far from Dome C. the ~~, and so the~~ record of eruptions is therefore likely dominated by those that have reached the stratosphere and have a global climate effect.

Eruptions can be logged using spikes in sulfate, or as a surrogate, spikes in the dielectric profile conductance (DEP) or low frequency electrical conductivity (ECM) of ice (Wolff, 2000), both of which respond to acidity in the ice. Such records are available continuously from a number of ice cores on the East Antarctic plateau. Issues of resolution and diffusion mean that the volcanic spikes cannot be reliably observed to the bottom of the cores, but they are clearly identified over at least the last two glacial cycles. This has for example allowed their use to synchronise age models to 128 ka bp between EPICA cores at Dome C (EDC) and Dronning Maud Land (EDML) (Ruth et al., 2007), to 145 ka between EDC and Vostok (Parrenin et al., 2012), and to 216 ka between EDC and Dome F (Fujita et al., 2015).

Several issues make it challenging to construct a consistent record of sulfate deposition throughout an ice core. Firstly, there is a background of sulfate from non-volcanic sources (mainly sea salt and marine biogenic). Because this background, and its variability, changes with climate, methods which merely seek outliers (Castellano et al., 2004) risk recording volcanic events

2

64 depositing a particular amount of sulfate in some climate periods and not in others. Secondly there is a very large amount of

65 variability in the amount of sulfate deposited in the small footprint of snow surface sampled by an ice core (Gautier et al.,

66 2016; Wolff et al., 2005), so that the sulfate signal of individual eruptions in a single core is subject to great uncertainty.

67 Thirdly, despite the lower frequency of local eruptions, Antarctic ice cores will still record some of these minor eruptions

68 which did not reach the stratosphere but are smaller eruptions of more regional origin. These can in principle be filtered using

69 sulfur isotope analysis to identify mass independent fractionation (Baroni et al., 2008; Burke et al., 2019; Gautier et al., 2019;

70 McConnell et al., 2017; Savarino et al., 2003a).

71 A final issue is related to resolution and diffusion. Snow accumulation rates at the East Antarctic sites mentioned above (Dome

72 Fuji, EDC, Vostok and EDML) vary from 2-6 cm water equivalent at the different sites in the present day and are typically

73 less than 50% of that in the last glacial maximum. Eruption signals are generally recorded above background for only 2-3

74 years. It is therefore essential to use only data with a good depth resolution (at EDC resolution of better than 5 cm is optimal),

75 and to estimate the flux across the peak and not just at the maximum, which will certainly be modulated by the resolution.

76 Additionally sulfate peaks diffuse with age (Barnes et al., 2003), and we find that volcanic peaks that were just a few years

77 wide on deposition may appear to be 20 years wide in ice of 200 ka age at EDC. This is helpful because it means that, as layers

78 thin with depth, the decreasing age resolution of our measurements is not a limiting factor. However it makes it yet more

79 challenging to identify eruptions of a particular scale in a consistent way, because peaks that stand clearly above background

80 in recent ice diffuse towards the background in older ice.

81 It is also important to be aware that even a perfect record of sulfate deposition events is not easy to convert into a record of

82 eruption magnitude and frequency. In addition to the strength of the eruption, sulfate deposition depends on the sulfur content

83 of the eruption, the latitude of the volcano and atmospheric transport processes (Marshall et al., 2021). Finally, there are

84 difficulties in converting sulfate loading in an ice core to the magnitude (defined by volcanologists as magma mass erupted).

85 Eruption magnitude is only one of several factors that influence sulfate mass released in explosive eruptions (Wallace and

86 Edmonds, 2011).

87 Despite these problems two recent papers (Cole-Dai et al., 2021; Lin et al., 2022) have attempted to assess eruption frequency.

88 One (Cole-Dai et al., 2021) examined the number of eruptions recorded in the WAIS Divide core over the last 11 kyr, observing

89 variability but no trend in eruption rate. A second (Lin et al., 2022) assessed eruption frequencies recorded in both Greenland

90 and Antarctica over the period from 9-60 kyr ago, and compared them with the rates in the last 2 kyr. For Greenland they

91 found relatively constant rates of eruption through time, but with a small increase in frequency of recorded eruptions across

92 the deglaciation (21-9 ka). This is consistent with the idea that the removal of ice from high latitude eruption regions, with a

93 particular emphasis on Iceland (Jull and McKenzie, 1996), would have led to an increased eruption rate recorded in Greenland.

94 For Antarctica, using methods similar to those we describe later, the authors (Lin et al., 2022) found no significant change in

95 eruption rate across the 60 kyr period.

96 In this paper we log eruption frequencies from the Antarctic ice core of EDC to 200 ka, using a methodology that assesses the

97 scale of sulfate deposition consistently with depth, age and climate period. We use this to assess the variability in recorded

98 eruptions with time and with climate. We discuss how representative the eruption record in Antarctica is, and use sulfur isotope

99 analysis to augment this discussion.

2. Data

101 Sulfate was measured along the EPICA Dome C (EDC) ice core by two methods, standard ion chromatography (IC) and fast

102 ion chromatography (FIC) (Littot et al., 2002; Severi et al., 2015). FIC measurements were at higher resolution (typically 5-6

103 cm in the top 100 m, 3-5 cm below that to 770 m, and 2 cm below 770 m) than IC measurements; additionally there are sections

104 of the core where IC data are not available. For these reasons FIC data were preferred.

105 However, although initial tests had suggested good agreement between the methods (Littot et al., 2002), a more detailed

106 analysis suggested some calibration problems during the first field season of FIC use, to a depth of 358.6 metres (11745 years

107 before present (1950) on the AICC2012 age model). In this depth range we consider the well-established IC method to be more

108 reliable. Detailed comparison of FIC and IC data was carried out where both were available. While it is impossible to diagnose

109 exactly what the issue was, a plot of FIC data against IC data for values more than 50 µg kg^{-1} above the background showed a

110 gradient of 0.70 for data between 0 and 358.6 m, and 0.94 between 360 m and 720 m. This is shown in Fig. 1 and was used as

111 justification to multiply the FIC values above background (i.e. the residual after subtracting the background) by (1/0.7) for

112 data above 358.6 m (<11.7 ka) during the data processing.
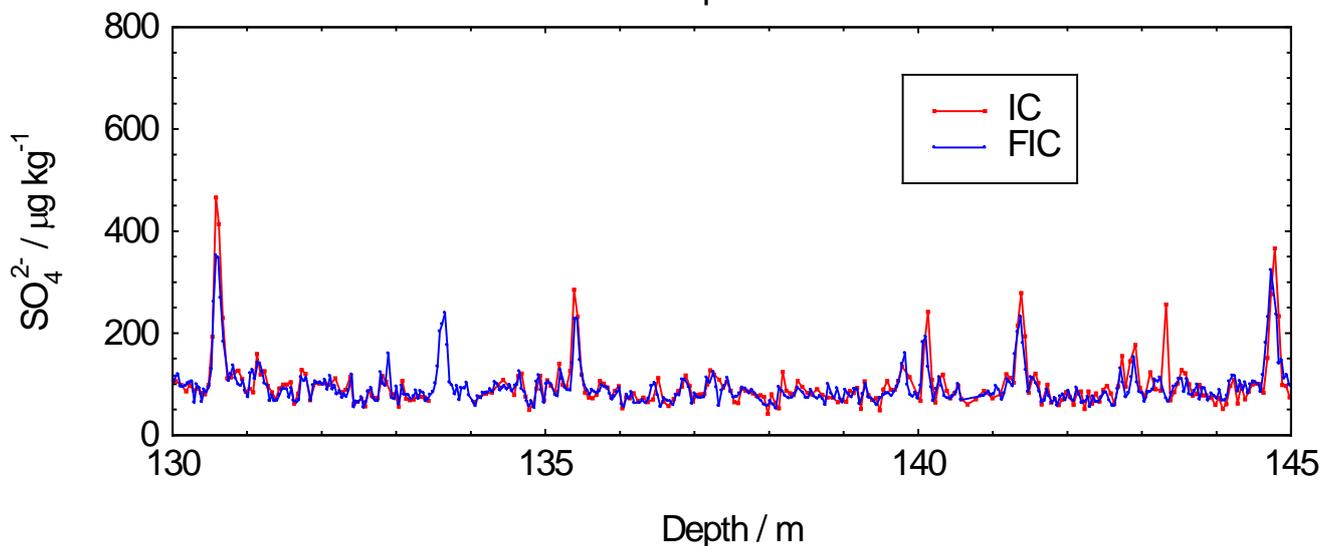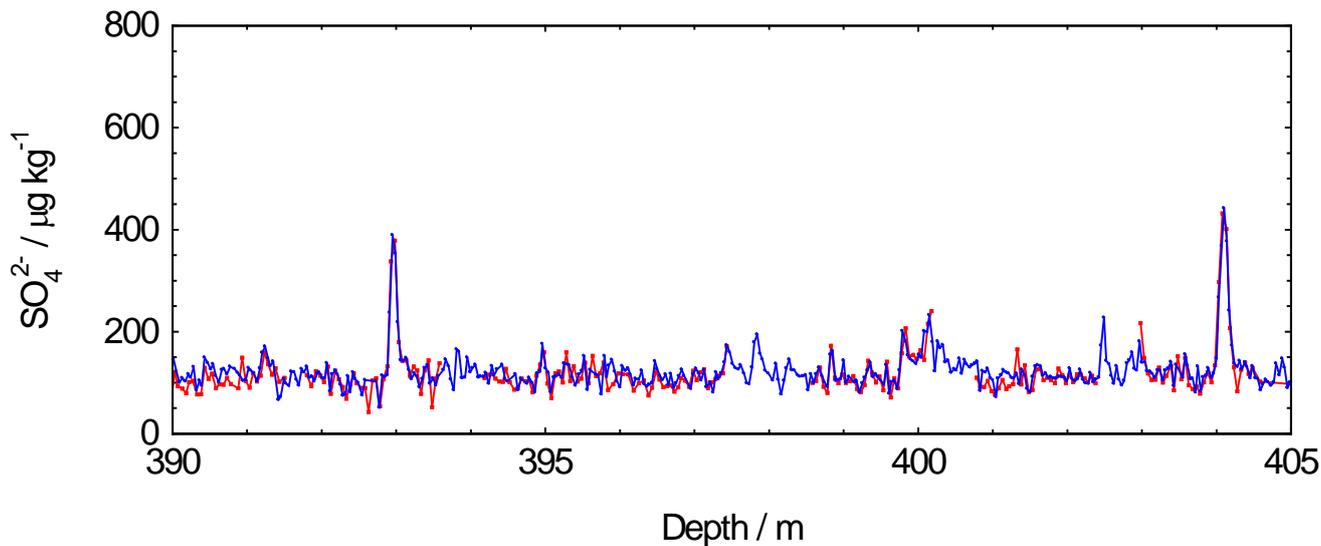
Figure 1. Comparison of FIC and IC data for two sections of the EDC ice core. In the section from 130 to 145 m, FIC peaks are consistently lower than those of IC while in the section from 390 metres, the concentrations are essentially the same in the two methods.

Beyond 358.6 m, the data were used without correction. Volcanic peaks, standing clear of the sulfate background, remain visible beyond 200 ka. It is clear that diffusion has occurred, making peaks considerably wider in years (and consequently smaller in amplitude) than they were at the time of deposition; however, thinning seems to balance diffusion rather closely (Fig. 2). The result is that peaks remain within about a 30 cm window at all depths to 200 ka, and the resolution of the data remains adequate to estimate peak areas.
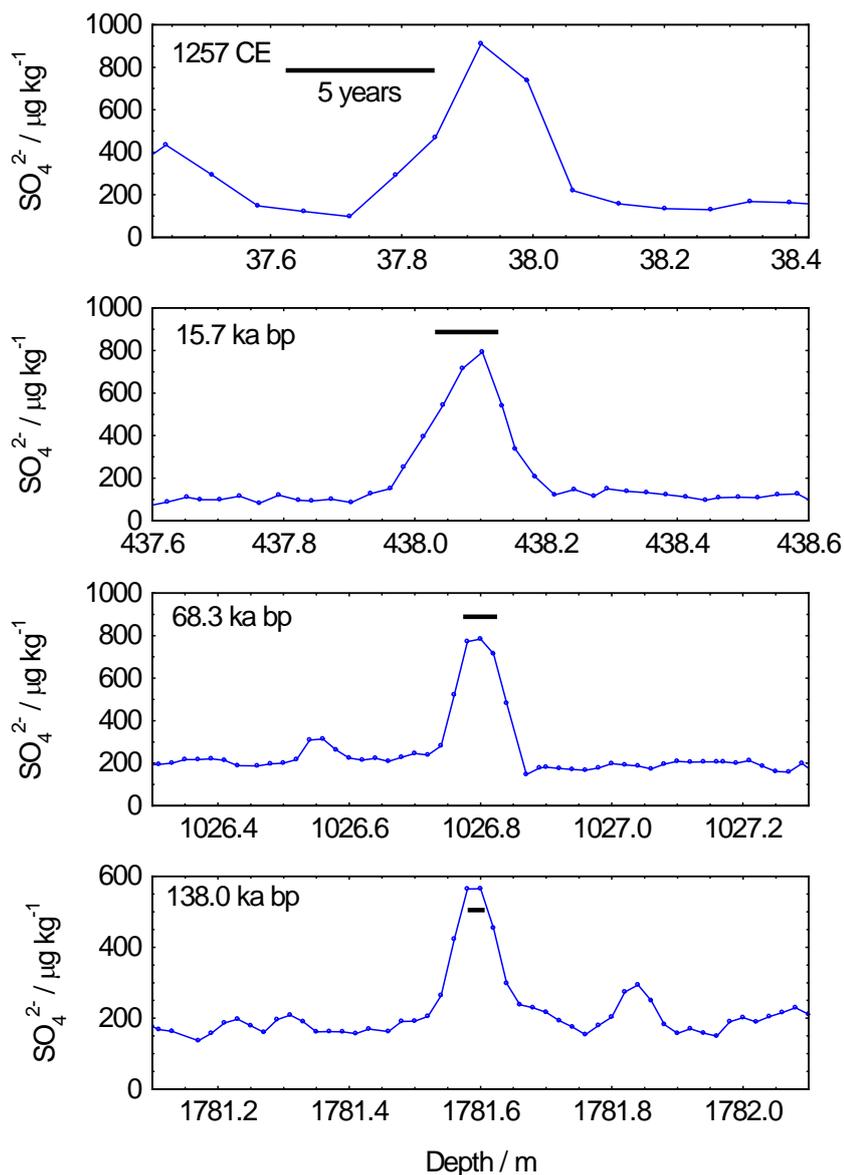
Figure 2. Examples of volcanic peaks at different depths and ages. The 1257 peak (top panel) is shown after application of the correction described above. The black horizontal bar on each plot represents 5 years at each depth. Dots represent the mid-depths of individual samples.

The dataset includes sections of missing data, where no FIC sulfate data are available. Mainly this consists of short sections at the end of core lengths, but there are some longer sections where data were not taken either because of poor core quality or instrument problems. Out of 2070 m of ice, there are 25 gaps longer than 30 cm, consisting in total of 19 m of ice. We discuss our treatment of missing data under methods.

6

130   In deeper ice, it has been observed (Traversi et al., 2009) that anomalous spikes in sulfate concentration form through an as-

131   yet uncharacterised post-depositional process. In Fig. 3 we show clear examples of this artefact at about 400 ka; sulfate appears

132   to have been "sucked" from the surrounding background into a sharp peak. We observed signs of this behaviour as shallow as

133   2500 m (300 ka). To avoid any possibility of including such artefact peaks, we restrict our subsequent analysis to the past 200

134   kyr. This also avoids the problem that peaks become harder to distinguish from background with greater depth.
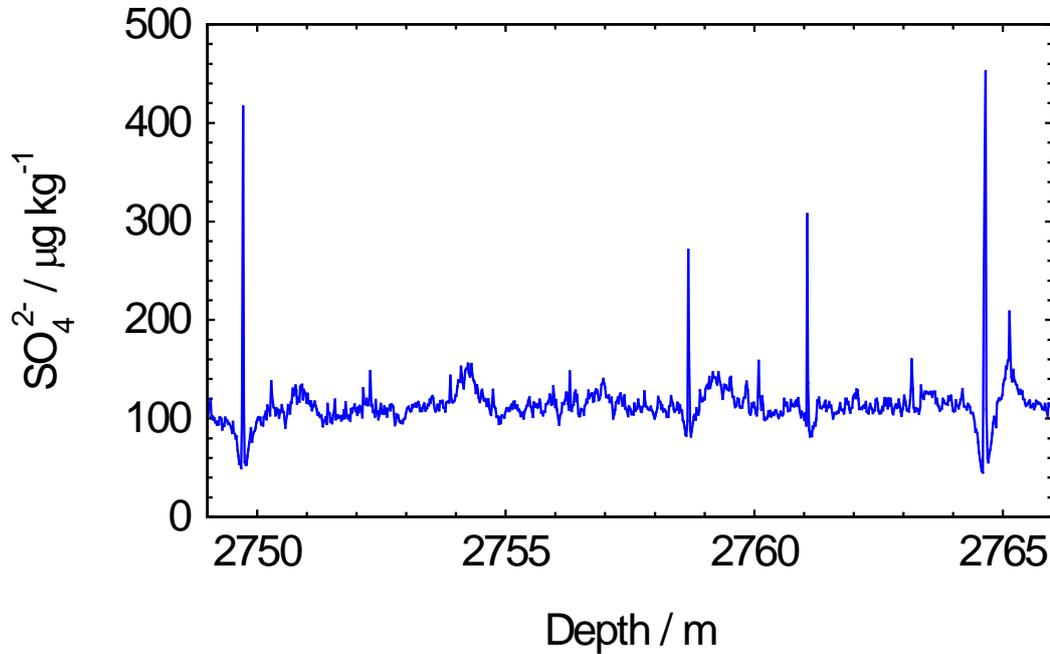
135

136   Figure 3. An example of four artefact peaks in ice aged just over 400 ka.

137   Material for the last few decades was not available in the EDC ice core because the top few metres were not retrieved. However,

138   the Pinatubo period has been studied previously at Dome C using snow pits (Castellano et al., 2005). The observed peak

139   (deposition of 10.7 mg m^{-2}) encompassed both Pinatubo and the eruption of Mount Hudson in Chile, which could not be

140   separated.   However, the two eruptions have been resolved at South Pole (Cole-Dai and Mosley-Thompson, 1999), allowing

141   a fraction of deposition in the combined peak to be assigned to each eruption. Using the same fraction, we estimate 7.5 mg m^{-}

142   ^{2} for the Pinatubo sulfate deposition at Dome C, used later as part of benchmarking our data.

143   **3.   Methods**

144   We applied the following method of calculating sulfate deposition. The ice core volcanic record consists of numerous sharp

145   spikes of sulfuric acid input, superimposed on a noisy background. The background consists mainly of sulfate from oxidation

146   of marine biogenic emissions of dimethylsulfide, with small contributions from sea salt as well as background volcanic sulfate.

147   Based on sulfate concentration measurements (Legrand and Delmas, 1984) and measurements of $\delta^{34}S$ in ice at South Pole

148   (Patris et al., 2000), the volcanic contribution to the background is estimated as less than 10%. In order to calculate the sulfate

149   deposition during each individual eruption event, we subtract the background and then sum the area across the peak, correcting

150   for ice thinning.

151   To correct for the background, we subtracted a running median from the dataset. The median is preferred to the mean because

152   the mean includes the volcanic peaks while the median should, if well-chosen, exclude the peaks. The time period over which

153   the median is calculated needs to be short enough that it follows the varying background but long enough that it will never use

154   the values within volcanic peaks. In our standard calculations we used 200 years, but other periods were also tested in

155   sensitivity studies. Varying the period over which the median was calculated between 100 and 400 years changed the total

156   number of peaks above a threshold of 20 mg m^{-2} by up to 10% compared to the standard case (200 years) but did not affect the

157   profile of peaks with time.

158   Having subtracted the background, we calculate the total amount of sulfate deposited to the snow per unit area across the whole

159   eruption. A key assumption is that the sulfate is mainly deposited by dry deposition, which is expected to be true at a site like

160   Dome C with its very low snow accumulation rate. This justifies the underlying assumption that the sulfate flux scales with

161   the amount of sulfate injected into the stratosphere. We first calculate the annual flux of sulfate in each sample (μg m^{-2} a^{-1}) as

162   $F = C * A$, where C is the concentration in a slice of ice (μg kg^{-1}), and A is the snow accumulation rate (kg m^{-2} a^{-1}). We then

163   calculate the total deposition in each sample (μg m^{-2}) by multiplying the flux by the time period represented in each sample;

164   this is done by using the accumulation rate and thinning parameter derived in the AICC2012 age model (Bazin et al., 2013) to

165   calculate the annual layer thickness. Finally, since the FIC data are effectively averages for discrete slices, we sum the

166   deposition (above background) in each of the samples that contribute to a particular peak to get the total deposition for an

167   individual eruption. This method automatically corrects the flux for the ice thinning (which is already 73% at the depth (2090

168   m) of 200 ka ice.

169   The algorithm we use searches for local maxima in the residual (after subtraction of the background) and calculates the sum

170   of samples across a chosen summing width across each maximum. The summing width needs to be large enough to include

171   all the volcanic sulfate after diffusion (Barnes et al., 2003). Visual observation suggests that a width of 30 cm (ie samples

172   within 15 cm of the concentration maximum) is appropriate at all depths between the surface and 2100 m (see Fig. 2). ThisThis

173   width is justified suggests thatbecause diffusion more or lessapproximately keeps pace with thinning at EDC. However, this

174   width was also varied in sensitivity studies. Varying the integration width between 20 and 40 cm altered the total number of

175   peaks above a threshold of 20 mg m^{-2} by up to 10% compared to the standard case (30 cm) but did not affect the profile of

176   peaks with time. At many depths, an integration width of 20 cm is clearly too narrow to capture the full peak, while 40 cm

177   includes sections of background, so the uncertainty induced by this parameter is below 10%.

178   Our method calculates numerous small peaks that are caused simply by variations around the background. To estimate this

179   variation we also calculate "negative" peaks around our median line. We then separately sum the number of peaks and negative

180   peaks in bins exceeding particular deposition fluxes (Figure 4). At a deposition of 10 µg m^{-2}, there is still a substantial number

181   of negative peaks (441 in 200 kyr, compared to 1518 positive peaks). At 20 mg m^{-2}, there are very few negative peaks (28 in

182   200 kyr compared to 678 positive peaks), suggesting that 96% of peaks we count at this level are volcanic eruption peaks, and

183   supporting our choice of 20 mg m^{-2} as the background threshold for counting peaks. There are no negative peaks at 40 mg m^{-}

184   ^{2}. This indicates that, while we could investigate volcanoes with lower deposition fluxes in some time periods, we should

185   restrict ourselves to peaks above 20 mg m^{-2} in order to count peaks of similar size consistently over 200 kyr.

186   In our standard calculation we treated missing data as having the concentration of the background, i.e. those sections did not

187   contribute to the size of volcanic peaks in which they were embedded. We also did a calculation where we set the value of all

188   missing sections less than 30 cm thick to be the average of the adjacent samples: this increased the total count of peaks > 20

189   mg m^{-2} by only 11 (out of 678). It is likely that the longer sections of missing data (25 sections > 30 cm, totalling 19 m of ice)

190   would have contained some peaks but assuming they contain the same proportion of volcanoes as the measured parts we have

191   probably missed less than 10 peaks with deposition >20 mg m^{-2}.
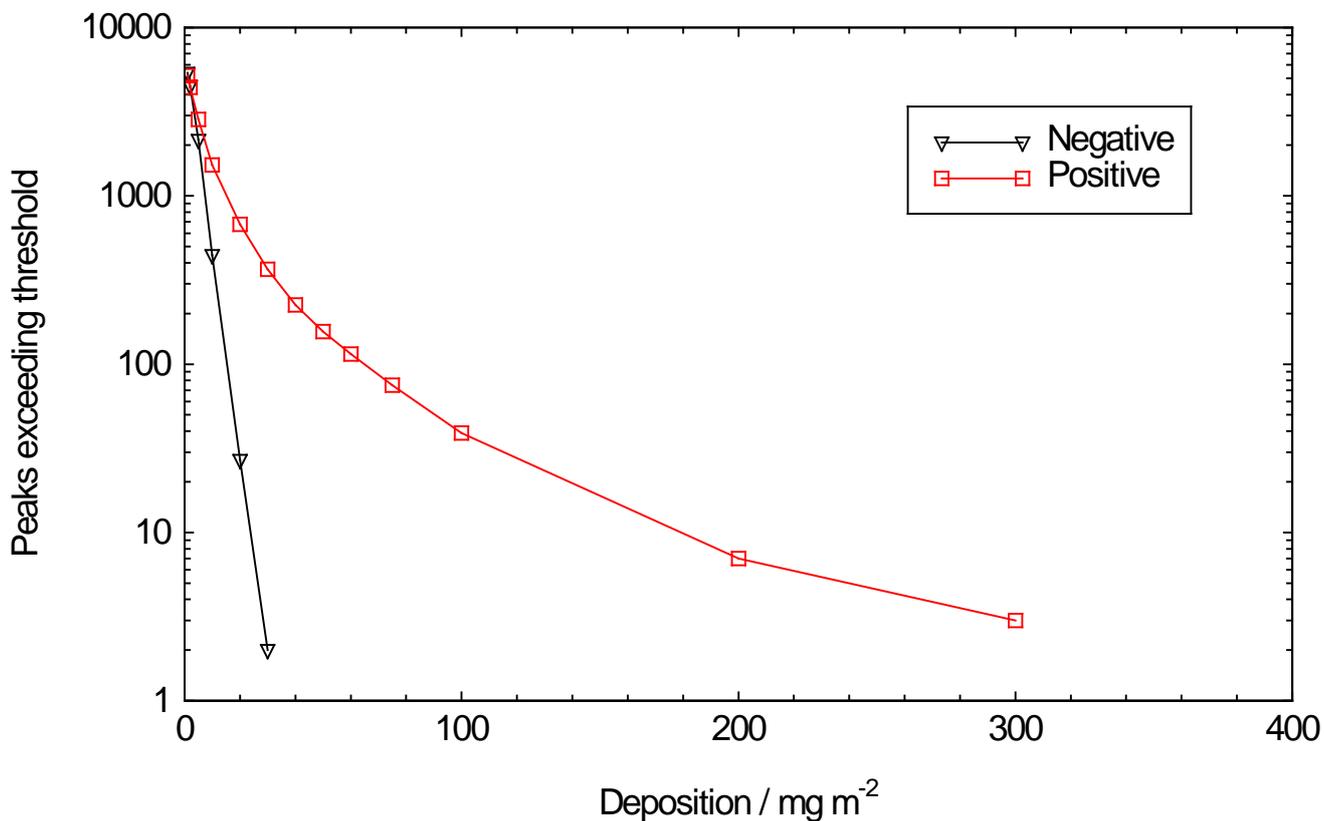
192

193   Figure 4. Distribution of positive and negative peaks exceeding different deposition fluxes, summed over the past 200 kyr.

194   Sulfur isotopes were measured on discrete samples of ice cut at high resolution (every 2-3 cm) across 21 volcanic sulfate

195   events from Dome C between 10.1 and 96.1 ka. These included examples of both larger and smaller volcanic peaks in the EDC

196   core. Samples were melted and measured for concentration by ion chromatography. Based on the concentration, a volume

197   corresponding to 20 nmol of sulfate was dried down and purified through anion exchange columns following the method

198   previously described (Burke et al., 2019). Each sample was measured at least twice for $\delta^{34}S$ and $\delta^{33}S$ by multi-collector

199   inductively coupled plasma mass spectrometry, where

200     $\delta^{x}S = (^{x}S/^{32}S)_{sample} / (^{x}S/^{32}S)_{reference} - 1$

201   and x is either 33 or 34. Mass independent fractionation was calculated as

202     $\Delta^{33}S = \delta^{33}S - ((\delta^{34}S + 1)*0.515 - 1)$

203   The uncertainty for these $\Delta^{33}S$ measurements is 0.14‰ (2 s.d.). Only sulfate that has been in the stratosphere shows a non-

204   zero signal of $\Delta^{33}S$, and so if the maximum magnitude $\Delta^{33}S$ across a peak is greater than 0.14‰, the eruption is considered

205   stratospheric.

206   **4.   The frequency of eruptions recorded in the EDC core, Antarctica**

207   A few of the most recent sulfate layers can be correlated to specific eruptions allowing some calibration of the record to the

208   magnitude of explosive eruptions (Gao et al., 2008; Sigl et al., 2015), but most layers cannot be linked to a source. As a

209   benchmark Table 1 lists four sulfate peaks in Dome C where the eruption location and magnitude are also known, including

210   the 1991 Pinatubo eruptions (Castellano et al., 2005). The benchmark data (all from tropical eruptions) imply that peaks above

211   our chosen threshold of 20 mg m^{-2} are likely to be M>6.5 eruptions.

Eruption	Dome C deposition (mg m^{-2})	Magnitude	Emission (Tg SO_2)
Pinatubo 1991	7.5	6.1	18
Krakatoa 1883	13.2	6.4	19
Rinjani/Samalas 1257	74.5	7.0	119
Tambora 1815	53	7.0	56

212

213   Table 1. Identified sulfate peaks in Dome C with magnitude and estimated emission (Toohey and Sigl, 2017).

214   Various attempts have been made to derive SO_2 emissions (in Mt or Tg of S or SO_2) from ice core deposition (in mg m^{-2} of

215   sulfate) (Sigl et al., 2022). However this is difficult when there is only one ice core location, and the location of the eruption

216   is unknown. Model studies show that the ratio of deposition in Antarctica to emissions depends on latitude of eruption, the

217   height the plume reaches, and the time of year of the eruption (Marshall et al., 2021). As a rough estimate using emissions

218   values calculated in the literature (Toohey and Sigl, 2017) we can deduce that for tropical eruptions, SO_2 emissions in Tg SO_2

219 are about 1-2 times higher than our measured EDC depositions in mg m^{-2} (Table 1). However the factor should certainly be

220 increased if eruptions occurred at high northern latitudes (Marshall et al., 2021).

221 It was already noted (Sigl et al., 2013; Sigl et al., 2015) that most Icelandic eruptions (such as Laki in 1783 CE and Eldgja in

222 939 CE) that give large depositions in Greenland cannot be identified in Antarctic cores. However these eruptions are anyway

223 estimated to be below the magnitude we would associate with depositions above our chosen threshold of 20 mg m^{-2}. An

224 eruption at 44 BCE, which is prominent in Greenland records, was recently identified with the Alaskan Okmok eruption

225 (McConnell et al., 2020), which has been assigned a magnitude of 6.7. The most likely candidate for this eruption in our EDC

226 record has a deposition of 15 mg m^{-2}, identical to the value previously noted for this eruption in Antarctica (Sigl et al., 2015).

227 It is therefore likely that for eruptions at high northern latitudes our threshold is closer to M>7.

228 Using our base set of parameters (200 year median calculation, 30 cm summation of layers per volcano, missing values treated

229 as having background concentration), we find that the last 200 kyr contains 678 volcanic events with deposition rates greater

230 than 20 mg m^{-2} (Fig. 4); this gives an average of 3.4 per millennium. Although our method is identical in concept, we calculate

231 rather more peaks greater than 20 mg m^{-2} (2.87/ka vs 2.21/kyr) for the period 9-60 ka than that estimated for EDC by previous

232 work (Lin et al., 2022). This difference seems to arise because our method calculates higher integrals for smaller peaks,

233 suggesting that the difference is related to the way that the background is calculated and/or the way that we deal with the width

234 of each peak. This is supported by the fact that at the extreme of our parameter choices (20 cm peak widths, and 100 year

235 interval for calculating the median background) our estimates converge with those of the previous work (Lin et al., 2022).

236 There are only 76 peaks with fluxes larger than that of Rinjani/Samalas (1257), making this a 1 in 2500 year event. A time

237 series of all eruptions greater than 20 mg m^{-2} is shown in Fig. 5.

238 Our results are also consistent with independent estimates of the global magnitude-frequency relationship (Rougier et al.,

239 2018). Based on data shown in Table 4, sulfate peaks > 20 mg m^{-2} should have magnitudes ≥6.5 while sulfate peaks > 50 mg

240 m^{-2} should have magnitudes ≥ 7. The analysis of global terrestrial data (Rougier et al., 2018) gives an estimate of M ≥ 6.5

241 eruptions as 2.75/kyr (confidence interval (CI) 1.6-4.3) and an estimate of M ≥ 7 eruptions as 0.8/kyr (CI 0.48 to 1.47). Thus

242 the event rates based on sulfate events at > 20 mg m^{-2} (3.4/kyr) and > 50 mg m^{-2} (0.78/kyr) are well within the uncertainty

243 ranges of the estimates from the global terrestrial record.

244 The largest peaks in the past 200 kyr deposited around 300 mg m^{-2}. The largest recorded eruption in the timeframe that could

245 accommodate the Toba eruption (Crick et al., 2021; Svensson et al., 2013) has a flux of 133 mg m^{-2} (16th largest in our record),

246 Thus it unlikely that This raises questions as to whether, in terms of global dispersion of sulfate aerosol, Toba was the most

247 significant volcanic climate forcing event of the past 200 kyr. However additional data from other deep ice cores covering this

248 time period are needed to determine this more certainly.
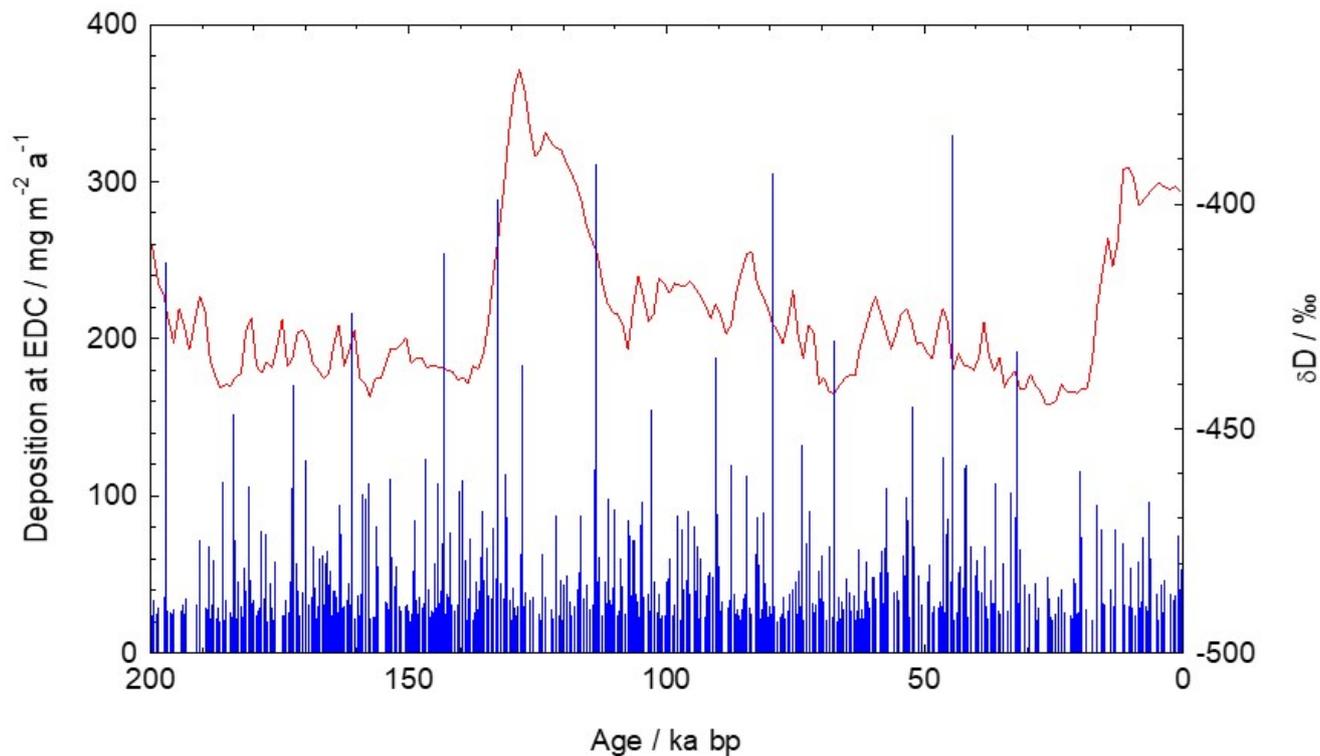
249

Figure 5. The deposition flux of sulfate for events with deposition more than 20 mg m^{-2} over the last 200 kyr (blue, left axis). Antarctic δD is shown in red (right axis) to indicate the climatic context..

To assess whether there are particular periods with high or low numbers of eruptions, we plot the cumulative number of large sulfate deposition events with time (Figure 6). Concentrating mainly on the result for eruptions greater than 20 mg m^{-2} because of the greater numbers involved, the trend is linear, indicating a steady state of large explosive eruptions across two glacial cycles. There is no sign of an increased slope (i.e., increased eruption frequency) at the two periods of deglaciation or interglacials. This can be seen in Fig. 7. The number of eruptions per millennium is very variable, as is to be expected from counting statistics for such small numbers. As a result the time series plot of the occurrence data is very scattered (Fig. 7). Nonetheless it is quite obvious that, at Dome C, both periods of deglaciation tend to have eruption frequencies at the lower end of the range, rather than increased rates.

260
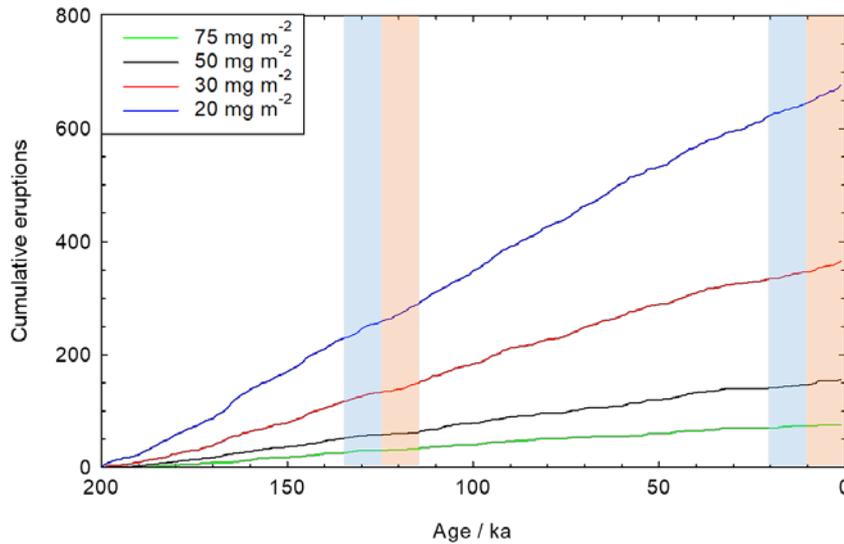
261

Figure 6: Cumulative eruption numbers over the past 200 kyr recorded in the Dome C ice core for different eruption deposition fluxes of sulfate. Periods of deglaciation marked with blue bar, interglacials with orange bar.


264
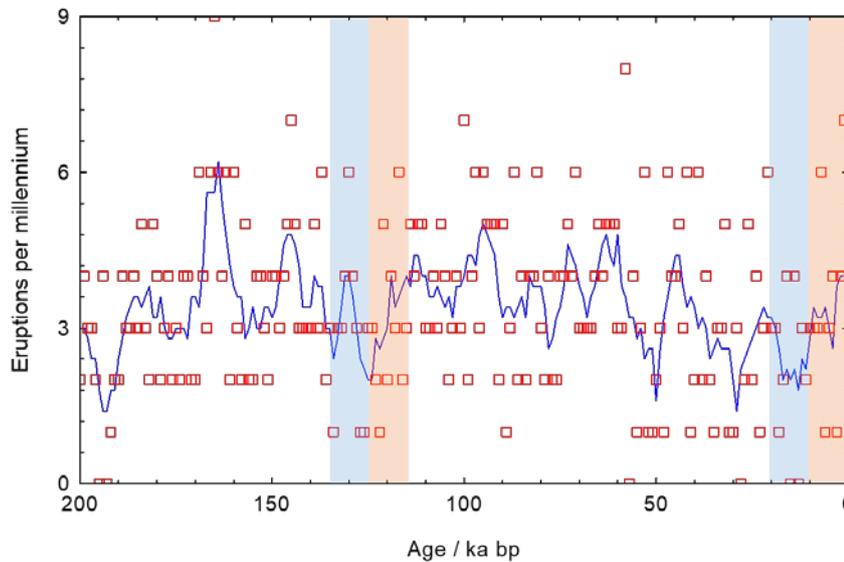
Figure 7: Eruption numbers per millennium (red) and 5 kyr running mean (blue). Periods of deglaciation marked with blue bar, interglacials with orange bar.

We explored other ways of analysing the ice core data to assess whether a climate cycle signal can be recognised. Using spectral analysis on the millennial eruption counts, we identified a possible peak corresponding to a 20 kyr period (frequency similar to precession) that emerges with weak statistical significance. This certainly needs to be confirmed in other records.

13

270 Although there have been weak indications of a 23 kyr period in Mediterranean tephra data (Kutterolf et al., 2019) it is difficult

271 to envisage a mechanism by which precession would influence global volcanism, given that it leads to much weaker changes

272 in ice sheet unloading and sea level compared to the longer (of order 100 kyr) period. Temperature and snow accumulation

273 rate at the EDC site show only very weak precessional power (Jouzel et al., 2007), so precessional changes in deposition

274 efficiency are unlikely to be strong. However, precession significantly influences tropical hydroclimate and the position and

275 width of the ITCZ (Singarayer et al., 2017). These changes could affect the washout of aerosol from eruptions in tropical

276 regions, and hence their ability to reach the stratosphere. There will certainly also be an associated effect on the efficiency of

277 the Brewer Dobson circulation that transports aerosol to the poles through the stratosphere, although we are not aware of model

278 simulations of this transport involving significant changes in precession (Fu et al., 2020). Thus, if the 20 kyr period is confirmed

279 it might be ascribed to a small change in the effectiveness of transporting tropical or Northern Hemisphere eruption material

280 to Antarctica. We emphasise that there is no significant signal at the lower Milankovitch frequency corresponding to 40 kyr.

281 Our record is too short to make a meaningful assessment in frequency space of the ~100 kyr cycle on which deglaciations

282 occur, but we again emphasise that, if anything, we see lower numbers of recorded events across the two deglaciations.

283 **5. Discussion**

284 As described earlier, there are several challenges when interpreting this dataset as a record of global volcanism. First, there is

285 the difficulty of separating local tropospheric from larger magnitude stratospheric eruptions. Mass-independent sulfur isotopes

286 in ice cores can be used to determine whether a volcanic event was stratospheric (Baroni et al., 2008; Burke et al., 2019;

287 Gautier et al., 2019; Savarino et al., 2003b). Isotope analysis of large sulfate peaks from the last 2600 years at Dome C (Gautier

288 et al., 2019) indicates 11 tropospheric and 49 stratospheric events, with 4 events showing an inconclusive signal. All the

289 largest events (>20 mg m^{-2} deposited at Dome C) were stratospheric. In this study, we tested if the proportion of stratospheric

290 events recorded at Dome C was the same earlier in the record by measuring an additional 21 events from Dome C between

291 10.1 and 96.1 ka following previous methods (Burke et al., 2019). Mass-independent fractionation of S occurs when sulfur

292 dioxide is photo-oxidised above the ozone layer, producing positive values of Δ^{33}S, followed by (for reasons of mass balance)

293 negative values, so that non-zero values of either sign indicate material that has reached the stratosphere. We found (Fig. 8 and

294 supplementary table) that most (18 out of 21; 15 out of 17 for deposition >20 mg m^{-2}) volcanic signals in Dome C are

295 stratospheric, consistent with its isolated location away from most volcanic sources. The sulfur isotope data therefore show

296 that more than 80% of the volcanic events recorded at Dome C involved stratospheric input due to large explosive eruptions.
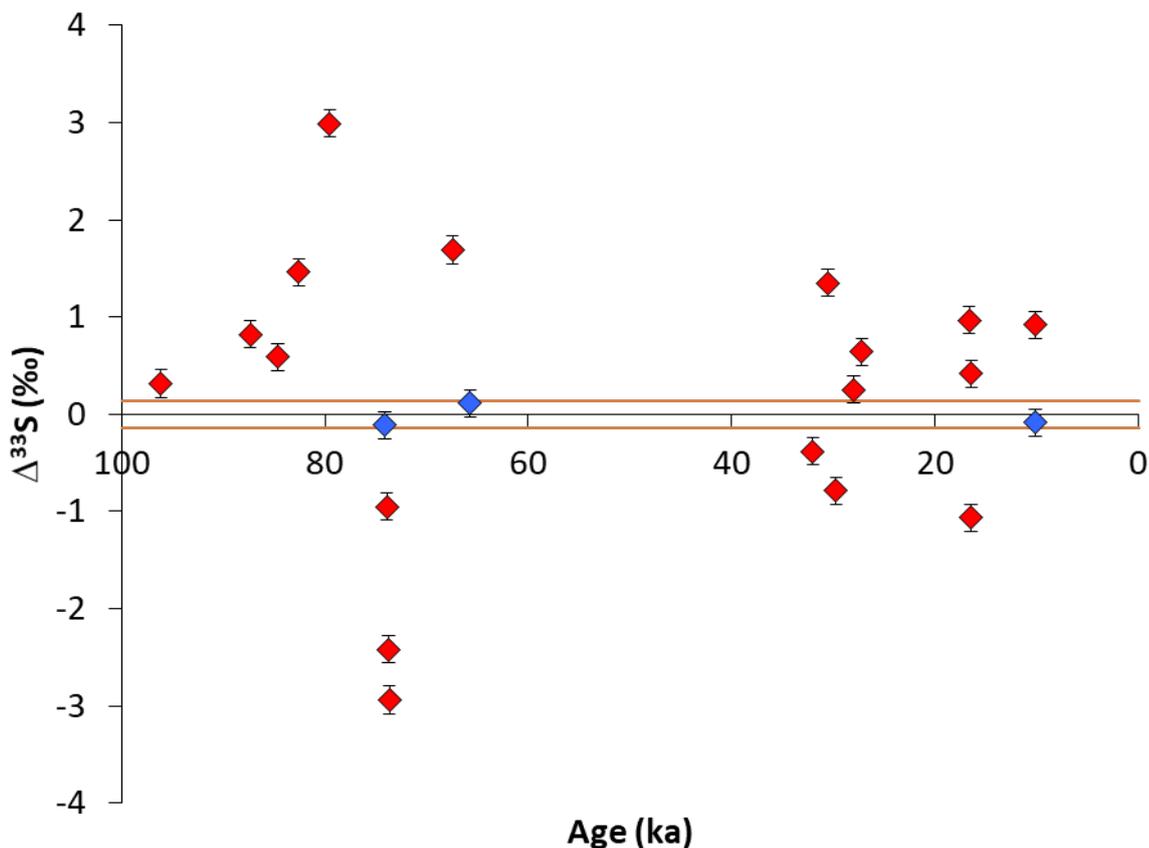
14

297

Fig. 8. Values of $\Delta^{33}S$ for 21 large volcanic eruptions recorded at Dome C in the last 100 kyr. Values outside a range of $\pm 0.14‰$ are considered to indicate a stratospheric eruption.

Second, sulfate peak amplitudes can vary strongly between core sites that are close together, and major peaks can even be missing at a single site (Gautier et al., 2016; Wolff et al., 2005). This problem is particularly pronounced at sites with low snow accumulation where years may be missing, like Dome C (Wolff et al., 2005), but these sites must be used to investigate long records of volcanism. This issue will cause variability in measured eruption rates which should average out over longer time periods.

Third, there will be a significant bias in the record of global explosive volcanism in Antarctica as a consequence of source locations and magnitude. Northern Hemisphere extratropical eruptions (>23°N) will be under-represented and biased towards very large eruptions with the likelihood of sulfate aerosol moving into the Southern Hemisphere being a function of source latitude and magnitude (Marshall et al., 2021). Thus the Antarctic volcanic record will be biased by larger depositional fluxes for tropical and especially Southern Hemisphere extratropical sources while exhibiting smaller depositional fluxes or even missing events for Northern Hemisphere extratropical eruptions.

15

311 The bias in source locations with extratropical Northern Hemisphere eruptions being underrepresented may result in net under-
312 recording. The estimates of Sigl et al. (Sigl et al., 2015) suggest that around 80% of eruptions giving the greatest global aerosol
313 loadings are recorded in Antarctica. Our Antarctic ice core data therefore might underestimate the number of eruptions in each
314 size class by perhaps 20%, somewhat compensated by the ~20% of eruptions from regional volcanoes recorded in Antarctica
315 that are tropospheric (Gautier et al., 2019). To first order, both the over-recording due to tropospheric eruptions and the under-
316 recording of extratropical northern hemisphere eruptions should operate in a similar way through time (excluding any effects
317 of changing transport strength discussed above) and across a range of eruption magnitudes. Thus the shape of the plots of
318 number of eruptions versus time and of number against sulfur deposition should be unaffected.

319 Finally the ice core record in Antarctica is a record of large silicic explosive eruptions (likely mostly M > 6.5). A spatial
320 analysis of the LaMEVE database of Quaternary explosive eruptions (Fig. 1 in Brown et al., 2014) show that the sources of
321 these big eruptions are largely in low and mid latitudes. This spatial bias is a consequence of present day plate boundary
322 distributions. Tectonic settings conducive to forming large silicic magma reservoirs and characterised by caldera forming large
323 magnitude explosive eruptions are typically in low and mid latitudes where deglaciation effects on melt generation are likely
324 to be absent or greatly reduced. There are no known M>7 Quaternary eruption from a northern high latitude volcano (>60°N)
325 (Brown et al., 2014). Thus our findings are not necessarily in contradiction to previous findings (such as Huybers and
326 Langmuir, 2009) because the Antarctic record is biased towards silicic explosive eruption in the southern hemisphere and
327 tropical regions.

328 **6.   Conclusions**

329 In this study we have extended the study of explosive eruptions recorded at the EDC ice core to 200 ka BP, using a method
330 that should consistently record large volcanic events through time. The record mainly represents large magnitude explosive
331 eruptions with magnitudes of 6.5 or above. We find no systematic variability through time, though there could be a small effect
332 of transport efficiency manifested in an apparent 20 kyr period that needs to be confirmed in other cores. There is no sign of
333 any increase in eruption frequency at deglaciations. This does not of course negate the likelihood that unloading of ice did
334 cause increased frequencies in regions susceptible to such effects, such as Iceland. However, taking into account the S isotope
335 evidence that most large eruptions recorded at EDC are stratospheric, our record is probably representative for the major events
336 influencing climate through stratospheric sulfate. We cannot rule out an effect from volcanism on the balance of CO_2
337 production and removal at deglaciation (Huybers and Langmuir, 2009), but it would have to operate only through smaller high
338 latitude eruptions and/or submarine volcanism. Finally we comment that it is difficult to study volcanism in ice cores over a
339 period longer than 200 ka until the post-depositional effects leading to artefact peaks are better understood.

340 **Data availability**

The sulfate data on which this paper is based are available at the NCEI paleoclimate data center, at https://www.ncdc.noaa.gov/paleo-search/study/31332; the depths and ages of large volcanic peaks in the EDC ice core that form the basis for Figures 5-7 are listed at Wolff, Eric W; Severi, Mirko (2021): Fluxes of largest volcanic peaks in the EDC sulfate record. PANGAEA, https://doi.org/10.1594/PANGAEA.926087

The age model data, including accumulation rate and thinning factor, is available in the supplement to the Bazin et al. (2013) and in the Pangaea database at https://doi.org/10.1594/PANGAEA.824865

The code used to identify, sum and count peaks, as well as the input data file, is attached as a supplement to this paper.

Author contribution

EW, AB and RSJS conceived the idea for this paper. MS provided the sulfate data that were analysed by the Firenze laboratory. EW and SHM studied the ice core data to determine which samples should undergo S isotope analysis. SHM, EAD and LC prepared the samples for S isotope analysis, while AB, HMI and LC carried out those analyses. EWW developed and implemented the sulfate peak identification method, analysed and sensitivity tested the data. AB and JWBR investigated the spectral properties of the data. RSJS and SHM advised about the nature of the volcanic record, including marine and terrestrial data. RSJS, EWW and AB prepared sections of text and all authors edited the text.

Competing interests

One of the authors is a member of the CP editorial board. The authors declare that they have no other conflicts of interest.

Figure captions

Figure 1. Comparison of FIC and IC data for two sections of the EDC ice core. In the section from 130 to 150 m, FIC peaks are consistently lower than those of IC while in the section from 390 metres, the concentrations are the same in the two methods.

Figure 2. Examples of volcanic peaks at different depths and ages. The 1257 peak (top panel) is shown after application of the correction described above. The black horizontal bar on each plot represents 5 years at each depth. Dots represent the mid-depths of individual samples.

Figure 3. An example of four artefact peaks in ice aged just over 400 ka.

Figure 4. Distribution of positive and negative peaks exceeding different deposition fluxes, summed over the past 200 kyr.

Figure 5. The deposition flux of sulfate for events with deposition more than 20 mg m^{-2} over the last 200 kyr.

Figure 6: Cumulative eruption numbers over the past 200 kyr recorded in the Dome C ice core for different eruption deposition fluxes of sulfate. Periods of deglaciation marked with blue bar, interglacials with orange bar.

Figure 7: Eruption numbers per millennium (red) and 5 kyr running mean (blue). Periods of deglaciation marked with blue bar, interglacials with orange bar.

Fig. 8. Values of $\Delta^{33}S$ for 21 large volcanic eruptions recorded at Dome C in the last 100 kyr. Values outside a range of ±0.14‰ are considered to indicate a stratospheric eruption.

References

Barnes, P. R. F., Wolff, E. W., Mader, H. M., Udisti, R., Castellano, E., and Rothlisberger, R.: Evolution of chemical peak shapes in the Dome C, Antarctica, ice core, J. Geophys. Res., 108, doi:10.1029/2002JD002538, 2003.

Baroni, M., Savarino, J., Cole-Dai, J. H., Rai, V. K., and Thiemens, M. H.: Anomalous sulfur isotope compositions of volcanic sulfate over the last millennium in Antarctic ice cores, J. Geophys. Res.-Atmos., 113, doi: 10.1029/2008jd010185, 2008.

Bazin, L., Landais, A., Lemieux-Dudon, B., Kele, H. T. M., Veres, D., Parrenin, F., Martinerie, P., Ritz, C., Capron, E., Lipenkov, V., Loutre, M. F., Raynaud, D., Vinther, B., Svensson, A., Rasmussen, S. O., Severi, M., Blunier, T., Leuenberger, M., Fischer, H., Masson-Delmotte, V., Chappellaz, J., and Wolff, E. W.: An optimised multi-proxy, multi-site Antarctic ice and gas orbital chronology (AICC2012): 120-800 ka, Climate of the Past 9, 1715-1731, 2013.

Brown, S. K., Crosweller, H. S., Sparks, R. S. J., Cottrell, E., Deligne, N. I., Guerrero, N. O., Hobbs, L., Kiyosugi, K., Loughlin, S. C., Siebert, L., and Takarada, S.: Characterisation of the Quaternary eruption record: analysis of the Large Magnitude Explosive Volcanic Eruptions (LaMEVE) database, Journal of Applied Volcanology, 3, 5, doi: 10.1186/2191-5040-3-5, 2014.

Burke, A., Moore, K. A., Sigl, M., Nita, D. C., McConnell, J. R., and Adkins, J. F.: Stratospheric eruptions from tropical and extra-tropical volcanoes constrained using high-resolution sulfur isotopes in ice cores, Earth planet. Sci. Lett., 521, 113-119, doi: https://doi.org/10.1016/j.epsl.2019.06.006, 2019.

Castellano, E., Becagli, S., Hansson, M., Hutterli, M., Petit, J. R., Rampino, M. R., Severi, M., Steffensen, J. P., Traversi, R., and Udisti, R.: Holocene volcanic history as recorded in the sulfate stratigraphy of the European Project for Ice Coring in Antarctica Dome C (EDC96) ice core, J. Geophys. Res., 110, D06114, doi:06110.01029/02004JD005259, 2005.

Castellano, E., Becagli, S., Jouzel, J., Migliori, A., Severi, M., Steffensen, J. P., Traversi, R., and Udisti, R.: Volcanic eruption frequency over the last 45 ky as recorded in Epica-Dome C ice core (East Antarctica) and its relationship with climatic changes, Global and Planetary Change, 42, 195-205, 2004.

Cole-Dai, J., Ferris, D. G., Kennedy, J. A., Sigl, M., McConnell, J. R., Fudge, T. J., Geng, L., Maselli, O. J., Taylor, K. C., and Souney, J. M.: Comprehensive Record of Volcanic Eruptions in the Holocene (11,000 years) From the WAIS Divide, Antarctica Ice Core, Journal of Geophysical Research: Atmospheres, 126, e2020JD032855, doi: https://doi.org/10.1029/2020JD032855, 2021.

Cole-Dai, J. and Mosley-Thompson, E.: The Pinatubo eruption in South Pole snow and its potential value to ice-core paleovolcanis records, Ann. Glaciol., 29, 99-105, 1999.

Crick, L., Burke, A., Hutchison, W., Kohno, M., Moore, K. A., Savarino, J., Doyle, E. A., Mahony, S., Kipfstuhl, S., Rae, J. W. B., Steele, R. C. J., Sparks, R. S. J., and Wolff, E. W.: New insights into the ~ 74ka Toba eruption from sulfur isotopes of polar ice cores, Clim. Past, 17, 2119-2137, doi: 10.5194/cp-17-2119-2021, 2021.

Fu, Q., White, R. H., Wang, M., Alexander, B., Solomon, S., Gettelman, A., Battisti, D. S., and Lin, P.: The Brewer-Dobson Circulation During the Last Glacial Maximum, Geophys. Res. Lett., 47, e2019GL086271, doi: https://doi.org/10.1029/2019GL086271, 2020.

Fujita, S., Parrenin, F., Severi, M., Motoyama, H., and Wolff, E. W.: Volcanic synchronization of Dome Fuji and Dome C Antarctic deep ice cores over the past 216 kyr, Clim. Past, 11, 1395-1416, doi: 10.5194/cp-11-1395-2015, 2015.

Gao, C., Robock, A., and Ammann, C.: Volcanic forcing of climate over the past 1500 years: An improved ice core-based index for climate models, J. Geophys. Res., 113, D23111, 2008.

Gautier, E., Savarino, J., Erbland, J., Lanciki, A., and Possenti, P.: Variability of sulfate signal in ice core records based on five replicate cores, Climate of the Past, 12, 103-113, doi: 10.5194/cp-12-103-2016, 2016.

Gautier, E., Savarino, J., Hoek, J., Erbland, J., Caillon, N., Hattori, S., Yoshida, N., Albalat, E., Albarede, F., and Farquhar, J.: 2600-years of stratospheric volcanism through sulfate isotopes, Nature Communications, 10, 466, doi: 10.1038/s41467-019-08357-0, 2019.

Huybers, P. and Langmuir, C.: Feedback between deglaciation, volcanism, and atmospheric CO2, Earth planet. Sci. Lett., 286, 479-491, doi: 10.1016/j.epsl.2009.07.014, 2009.

Jouzel, J., Masson-Delmotte, V., Cattani, O., Dreyfus, G., Falourd, S., Hoffmann, G., Nouet, J., Barnola, J. M., Chappellaz, J., Fischer, H., Gallet, J. C., Johnsen, S., Leuenberger, M., Loulergue, L., Luethi, D., Oerter, H., Parrenin, F., Raisbeck, G., Raynaud, D., Schwander, J., Spahni, R., Souchez, R., Selmo, E., Schilt, A., Steffensen, J. P., Stenni, B., Stauffer, B., Stocker, T., Tison, J.-L., Werner, M., and Wolff, E. W.: Orbital and millennial Antarctic climate variability over the last 800 000 years, Science, 317, 793-796, doi: 10.1126/science.1141038, 2007.

Jull, M. and McKenzie, D.: The effect of deglaciation on mantle melting beneath Iceland, J. Geophys. Res.-Solid Earth, 101, 21815-21828, doi: 10.1029/96jb01308, 1996.

Kutterolf, S., Schindlbeck, J. C., Jegen, M., Freundt, A., and Straub, S. M.: Milankovitch frequencies in tephra records at volcanic arcs: The relation of kyr-scale cyclic variations in volcanism to global climate changes, Quat. Sci. Rev., 204, 1-16, doi: 10.1016/j.quascirev.2018.11.004, 2019.

Legrand, M. and Delmas, R. J.: The ionic balance of Antarctic snow: a 10-year detailed record, Atmos. Environ., 18, 1867-1874, doi: 10.1016/0004-6981(84)90363-9, 1984.

Lin, J., Svensson, A., Hvidberg, C. S., Lohmann, J., Kristiansen, S., Dahl-Jensen, D., Steffensen, J. P., Rasmussen, S. O., Cook, E., Kjær, H. A., Vinther, B. M., Fischer, H., Stocker, T., Sigl, M., Bigler, M., Severi, M., Traversi, R., and Mulvaney, R.: Magnitude, frequency and climate forcing of global volcanism during the last glacial period as seen in Greenland and Antarctic ice cores (60–9 ka), Clim. Past, 18, 485-506, doi: 10.5194/cp-18-485-2022, 2022.

Littot, G. C., Mulvaney, R., Rothlisberger, R., Udisti, R., Wolff, E. W., Castellano, E., de Angelis, M., Hansson, M., Sommer, S., and Steffensen, J. P.: Comparison of analytical methods used for measuring major ions in the EPICA Dome C (Antarctica) ice core, Ann. Glaciol., 35, 299-305, 2002.

Mahony, S. H., Barnard, N. H., Sparks, R. S. J., and Rougier, J. C.: VOLCORE, a global database of visible tephra layers sampled by ocean drilling, Scientific Data, 7, doi: 10.1038/s41597-020-00673-1, 2020.

468

469 Marshall, L. R., Schmidt, A., Johnson, J. S., Mann, G. W., Lee, L. A., Rigby, R., and Carslaw, K. S.: Unknown Eruption Source Parameters
470 Cause Large Uncertainty in Historical Volcanic Radiative Forcing Reconstructions, Journal of Geophysical Research: Atmospheres, 126,
471 e2020JD033578, doi: https://doi.org/10.1029/2020JD033578, 2021.

472

473 McConnell, J. R., Burke, A., Dunbar, N. W., Köhler, P., Thomas, J. L., Arienzo, M. M., Chellman, N. J., Maselli, O. J., Sigl, M., Adkins, J.
474 F., Baggenstos, D., Burkhart, J. F., Brook, E. J., Buizert, C., Cole-Dai, J., Fudge, T. J., Knorr, G., Graf, H.-F., Grieman, M. M., Iverson, N.,
475 McGwire, K. C., Mulvaney, R., Paris, G., Rhodes, R. H., Saltzman, E. S., Severinghaus, J. P., Steffensen, J. P., Taylor, K. C., and Winckler,
476 G.: Synchronous volcanic eruptions and abrupt climate change ~17.7 ka plausibly linked by stratospheric ozone depletion, Proceedings of
477 the National Academy of Sciences, 114, 10035-10040, doi: 10.1073/pnas.1705595114, 2017.

478

479 McConnell, J. R., Sigl, M., Plunkett, G., Burke, A., Kim, W. M., Raible, C. C., Wilson, A. I., Manning, J. G., Ludlow, F., Chellman, N. J.,
480 Innes, H. M., Yang, Z., Larsen, J. F., Schaefer, J. R., Kipfstuhl, S., Mojtabavi, S., Wilhelms, F., Opel, T., Meyer, H., and Steffensen, J. P.:
481 Extreme climate after massive eruption of Alaska's Okmok volcano in 43 BCE and effects on the late Roman Republic and Ptolemaic
482 Kingdom, Proc. Natl. Acad. Sci. U. S. A., 117, 15443-15449, doi: 10.1073/pnas.2002722117, 2020.

483

484 Parrenin, F., Petit, J.-R., Masson-Delmotte, V., Basile, I., Jouzel, J., Lipenkov, V., Rasmussen, S., Schwander, J., Severi, M., Udisti, R.,
485 Veres, D., Vinther, B., and Wolff, E. W.: Volcanic synchronisation between the EPICA Dome C and Vostok ice cores
486 (Antarctica) 0-145 kyr BP, Climate of the Past 8, 1031-1045, 2012.

487

488 Patris, N., Delmas, R. J., and Jouzel, J.: Isotopic signatures of sulfur in shallow Antarctic ice cores, J. Geophys. Res.-Atmos., 105, 7071-
489 7078, 2000.

490

491 Robock, A.: Volcanic eruptions and climate, Rev. Geophys., 38, 191-219, doi: doi:10.1029/1998RG000054, 2000.

492

493 Rougier, J., Sparks, R. S. J., Cashman, K. V., and Brown, S. K.: The global magnitude–frequency relationship for large explosive volcanic
494 eruptions, Earth planet. Sci. Lett., 482, 621-629, doi: https://doi.org/10.1016/j.epsl.2017.11.015, 2018.

495

496 Ruth, U., Barnola, J. M., Beer, J., Bigler, M., Blunier, T., Castellano, E., Fischer, H., Fundel, F., Huybrechts, P., Kaufmann, P., Kipfstuhl,
497 J., Lambrecht, A., Morganti, A., Oerter, H., Parrenin, F., Rybak, O., Severi, M., Udisti, R., Wilhelms, F., and Wolff, E. W.: "EDML1": A
498 chronology for the EPICA deep ice core from Dronning Maud Land, Antarctica, over the last 150,000 years, Climate of the Past, 3, 475-
499 484, 2007.

500

501 Savarino, J., Bekki, S., Cole-Dai, J. H., and Thiemens, M. H.: Evidence from sulfate mass independent oxygen isotopic compositions of
502 dramatic changes in atmospheric oxidation following massive volcanic eruptions, J. Geophys. Res., 108, 4671, 2003a.

503

504 Savarino, J., Romero, A., Cole-Dai, J., Bekki, S., and Thiemens, M. H.: UV induced mass-independent sulfur isotope fractionation in
505 stratospheric volcanic sulfate, Geophys. Res. Lett., 30, doi: 10.1029/2003gl018134, 2003b.

506

507 Severi, M., Becagli, S., Traversi, R., and Udisti, R.: Recovering Paleo-Records from Antarctic Ice-Cores by Coupling a Continuous Melting
508 Device and Fast Ion Chromatography, Analyt. Chem., 87, 11441-11447, doi: 10.1021/acs.analchem.5b02961, 2015.

509

510 Sigl, M., McConnell, J. R., Layman, L., Maselli, O., McGwire, K., Pasteris, D., Dahl-Jensen, D., Steffensen, J. P., Vinther, B., Edwards, R.,
511 Mulvaney, R., and Kipfstuhl, S.: A new bipolar ice core record of volcanism from WAIS Divide and NEEM and implications for climate
512 forcing of the last 2000 years, Journal of Geophysical Research: Atmospheres, 118, 1151-1169, doi: https://doi.org/10.1029/2012JD018603,
513 2013.

514

515 Sigl, M., Toohey, M., McConnell, J. R., Cole-Dai, J., and Severi, M.: Volcanic stratospheric sulfur injections and aerosol optical depth
516 during the Holocene (past 11500 years) from a bipolar ice-core array, Earth Syst. Sci. Data, 14, 3167-3196, doi: 10.5194/essd-14-3167-2022,
517 2022.

518

519 Sigl, M., Winstrup, M., McConnell, J. R., Welten, K. C., Plunkett, G., Ludlow, F., Buntgen, U., Caffee, M., Chellman, N., Dahl-Jensen, D.,
520 Fischer, H., Kipfstuhl, S., Kostick, C., Maselli, O. J., Mekhaldi, F., Mulvaney, R., Muscheler, R., Pasteris, D. R., Pilcher, J. R., Salzer, M.,
521 Schupbach, S., Steffensen, J. P., Vinther, B. M., and Woodruff, T. E.: Timing and climate forcing of volcanic eruptions for the past 2,500
522 years, Nature, 523, 543-+, doi: 10.1038/nature14565, 2015.

523

524 Singarayer, J. S., Valdes, P. J., and Roberts, W. H. G.: Ocean dominated expansion and contraction of the late Quaternary tropical rainbelt,
525 Scientific Reports, 7, 9382, doi: 10.1038/s41598-017-09816-8, 2017.
526
527 Svensson, A., Bigler, M., Blunier, T., Clausen, H. B., Dahl-Jensen, D., Fischer, H., Fujita, S., Goto-Azuma, K., Johnsen, S. J., Kawamura,
528 K., Kipfstuhl, S., Kohno, M., Parrenin, F., Popp, T., Rasmussen, S. O., Schwander, J., Seierstad, I., Severi, M., Steffensen, J. P., Udisti, R.,
529 Uemura, R., Vallelonga, P., Vinther, B. M., Wegner, A., Wilhelms, F., and Winstrup, M.: Direct linking of Greenland and Antarctic ice
530 cores at the Toba eruption (74 ka BP), Clim. Past, 9, 749-766, doi: 10.5194/cp-9-749-2013, 2013.
531
532 Toohey, M. and Sigl, M.: Volcanic stratospheric sulfur injections and aerosol optical depth from 500 BCE to 1900 CE, Earth Syst. Sci. Data,
533 9, 809-831, doi: 10.5194/essd-9-809-2017, 2017.
534
535 Traversi, R., Becagli, S., Castellano, E., Marino, F., Rugi, F., Severi, M., Angelis, M. d., Fischer, H., Hansson, M., Stauffer, B., Steffensen,
536 J. P., Bigler, M., and Udisti, R.: Sulfate Spikes in the Deep Layers of EPICA-Dome C Ice Core: Evidence of Glaciological Artifacts,
537 Environmental Science & Technology, 43, 8737-8743, doi: 10.1021/es901426y, 2009.
538
539 Wallace, P. J. and Edmonds, M.: The Sulfur Budget in Magmas: Evidence from Melt Inclusions, Submarine Glasses, and Volcanic Gas
540 Emissions, Reviews in Mineralogy and Geochemistry, 73, 215-246, doi: 10.2138/rmg.2011.73.8, 2011.
541
542 Watt, S. F. L., Pyle, D. M., and Mather, T. A.: The volcanic response to deglaciation: Evidence from glaciated arcs and a reassessment of
543 global eruption records, Earth-Sci. Rev., 122, 77-102, doi: 10.1016/j.earscirev.2013.03.007, 2013.
544
545 Wolff, E. W.: Electrical stratigraphy of polar ice cores: principles, methods, and findings. In: Physics of Ice Core Records, Hondoh, T. (Ed.),
546 Hokkaido University Press, Sapporo, 2000.
547
548 Wolff, E. W., Cook, E., Barnes, P. R. F., and Mulvaney, R.: Signal variability in replicate ice cores, J. Glaciol., 51, 462-468, 2005.
549
550